nature food

ARTICLES

https://doi.org/10.1038/s43016-021-00315-8

Check for updates

Programmable design of seed coating function induces water-stress tolerance in semi-arid regions

Augustine T. Zvinavashe[1,4], Julie Laurent[1,4], Manal Mhada[2], Hui Sun[1], Henri Manu Effa Fouda[1], Doyoon Kim[1], Salma Mouhib[2], Lamfeddal Kouisni[2,3] and Benedetto Marelli[1]✉

In semi-arid regions, water stress during seed germination and early seedling growth is the highest cause of crop loss. In nature, some seeds (for example, chia and basil) produce a mucilage-based hydrogel that creates a germination-promoting microenvironment by retaining water, regulating nutrient entry and facilitating interactions with beneficial microorganisms. Inspired by this strategy, a two-layered biopolymer-based seed coating has been developed to increase germination and water-stress tolerance in semi-arid, sandy soils. Seeds are coated with a silk/trehalose inner layer containing rhizobacteria and a pectin/carboxymethylcellulose outer layer that reswells upon sowing and acts as a water jacket. Using *Phaseolus vulgaris* (common bean) cultured under water-stress conditions in an experimental farm in Ben Guerir, Morocco, the proposed seed coating effectively delivered rhizobacteria to form root nodules, resulted in plants with better health and mitigated water stress in drought-prone marginal lands. A programmable seed coating technology has the potential to increase seed germination and water-stress tolerance in semi-arid, sandy soils.

In semi-arid regions, which constitute around 15% of the world's land, water is the determining factor for crop production[1] and water stress during seed germination and early seedling growth is the highest cause of crop loss[2], with dramatic impact on food security for 1 billion people that are threatened by desertification and already live in conditions of malnutrition[3].

For semi-arid soils, water-holding compounds such as hydrophilic and superabsorbent polymers can be applied to seeds, mixed into the soil or deposited on roots before planting to increase water retention and usage efficiency[4]. However, the application of these polymers is labour and energy intensive and often results in the release of synthetic plastics in the soil[5]. As a complementary approach, plant growth-promoting rhizobacteria (PGPRs) can be used to enhance plant health in conditions of water scarcity[6,7]. PGPRs are biofertilizers that interact with plant roots to increase availability of nutrients and phytohormones and enhance plant response to heat, saline soil and drought[8]. Some PGPRs, such as rhizobia, can infect legume roots to form symbiotic nodules that fix nitrogen, limiting the use of fertilizers and enhancing plant health in semi-arid regions[9]. Nonetheless, the use of PGPRs is limited by their low resistance to desiccation stress[10,11] and competition upon resuscitation with a diversity of microorganisms present in the soil environment (that is, the spermosphere)[12]. Together, these limitations hamper the integration of rhizobia in simple delivery systems—as seed coating technologies—that do not require the use of skills, agricultural practices and resources often not available in semi-arid regions of the world[13].

In nature, polysaccharides present in the seed coat of myxospermous species occupying arid environments (for example, *Salvia hispanica*, *Ocimum basilicum* and *Plantago ovata*) swell and extrude, upon sowing, a halo of mucilage that completely envelops the seed[14–16]. The extruded mucilage generates a growth-promoting spermosphere that retains water, regulates nutrient entry and facilitates interactions with PGPRs[14]. Seed mucilage is of increasing interest to the pharmaceutical, biomedical and food industries and is usually a composite of pectic, non-cellulosic and cellulosic polysaccharides[17]. In this study, we were inspired by the multifunctional coat of myxospermous seed to develop a seed coating technology with programmable function that creates a spermosphere that positively affects the seed niche and promotes water-stress resistance in semi-arid soils.

Results

Design of the seed coating. The coating consists of a two-layered structure (Fig. 1). A scanning electron microscope image of the dry two-layered coating deposited on the surface of a *Phaseolus vulgaris* seed is depicted in Fig. 1a. The inner layer (layer 1) is made of a 1:3 mixture (by weight) of silk fibroin and trehalose that contains *Rhizobium tropici* CIAT 899—referred to as *R. tropici* CIAT 899 onwards. Silk fibroin is a 395 kDa structural protein that is extracted from the *Bombyx mori* silk cocoon with a yield of 70–75% and is the main component of silk textile fibres[18,19]. Through a water-based process applicable also to silk waste—cocoons unsuitable for reeling, yarn waste and garnetted stock—silk fibroin can be regenerated in a water suspension and then easily applied to form coatings through dip-coating and spray-coating techniques[20]. The physical, mechanical, biological and biodegradation properties of silk fibroin can be modulated by controlling the protein secondary and tertiary structures (random coil, alpha helix and beta sheet) at the point of material assembly or with post-processing techniques (silk fibroin polymorphism)[21–25]. Silk fibroin is also known to preserve biological entities and biomolecules encapsulated in silk-based materials by providing a barrier to oxygen stress, and minimize contact with water[26]. Trehalose is a disaccharide ubiquitously used by natural organisms to impart osmoprotection and can act as carbon source for rhizobium[27–29]. The mixture of silk fibroin and trehalose enables layer 1 adhesion to the seed coat, preservation

[1]Department of Civil and Environmental Engineering, Massachusetts Institute of Technology, Cambridge, MA, USA. [2]AgroBiosciences Department (AgBS), Mohammed VI Polytechnic University (UM6P), Ben-Guerir, Morocco. [3]African Sustainable Agriculture Research Institute, Mohammed VI Polytechnic University (ASARI-UM6P), Laayoune, Morocco. [4]These authors contributed equally: Augustine T. Zvinavashe, Julie Laurent. ✉e-mail: bmarelli@mit.edu

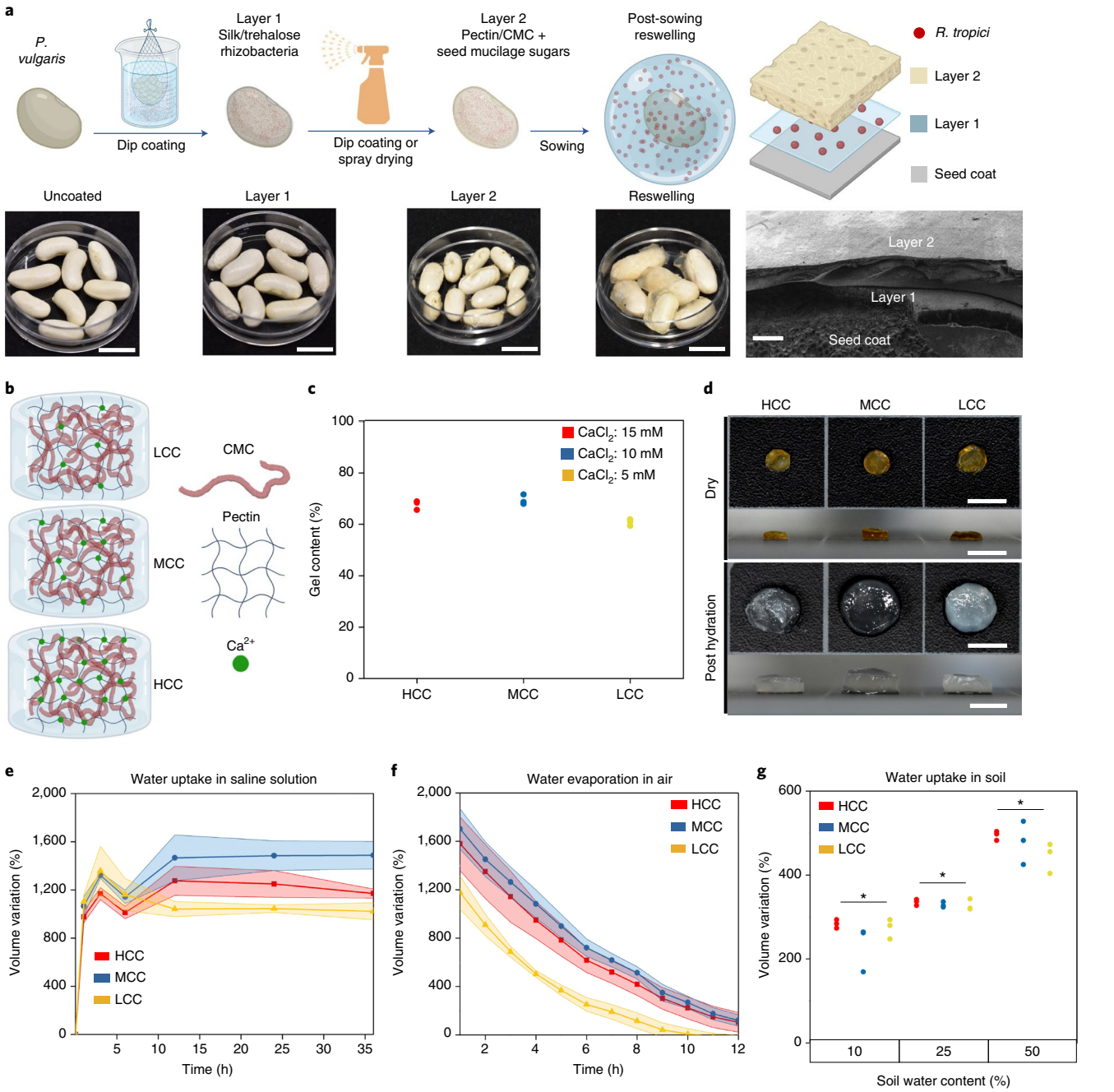

Fig. 1 | Material design, fabrication and selection. a, Schematic diagram of the two-layered seed coating fabrication process, relative pictures of *P. vulgaris* coated seeds and cross-section of coated seeds. Layer 1 contains a 1:3 mixture of silk/trehalose that adheres on the silk coat, encapsulates, preserves and releases *R. tropici* CIAT 899. Layer 2 is made of a 1:1 mixture of pectin/CMC (P:C). When the seed is watered, layer 2 swells into a hydrogel and hydrates layer 1, which dissolves and releases *R. tropici* CIAT 899. The hydrogel provides an appropriate environment for *R. tropici* CIAT 899 resuscitation and growth. Scale bars for pictures, 10 mm; scale bar for the scanning electron microscope image of the coating, 10 µm. **b**, Schematic of the pectin/CMC hydrogel structure, where Ca^{2+} at high, medium and low concentrations (HCC, MCC and LCC, respectively) are used to crosslink pectin chains while CMC acts as a filler to enhance water uptake. **c**, Effects of Ca^{2+} concentrations on gel content. Points of the same colour represent replicates. **d**, Representative images of dry and swollen (12 h in 154 mM NaCl solution) hydrogels. Scale bars, 10 mm. **e**, Water uptake over time of dried P:C in 154 mM NaCl solution. **f**, Water evaporation (in air) over time of hydrogels after a 12 h immersion in 154 mM NaCl solution. Highlighted areas around curves correspond to the standard error of the mean. **g**, Water uptake of P:C hydrogels in soils of increasing moisture content after 24 h. Stars above bars indicate a statistically significant difference in the mean swelling ratio of a soil moisture group compared with all other groups ($^*P < 0.05$). No statistically significant difference was found in the mean swelling ratios between $CaCl_2$ concentrations at similar soil moisture. Points of the same colour represent replicates.

of *R. tropici* CIAT 899 by mitigating oxidative and osmotic stresses, and release of the biofertilizer upon sowing[26,29,30]. Given layer 1 coating thickness (t), an ellipsoidal seed shape (a, b, c), the known concentration of *R. tropici* CIAT 899 (C_a) and assuming a homogeneous dispersion of *R. tropici* CIAT 899 and the formation of a homogeneous coating, it is possible to estimate the number of

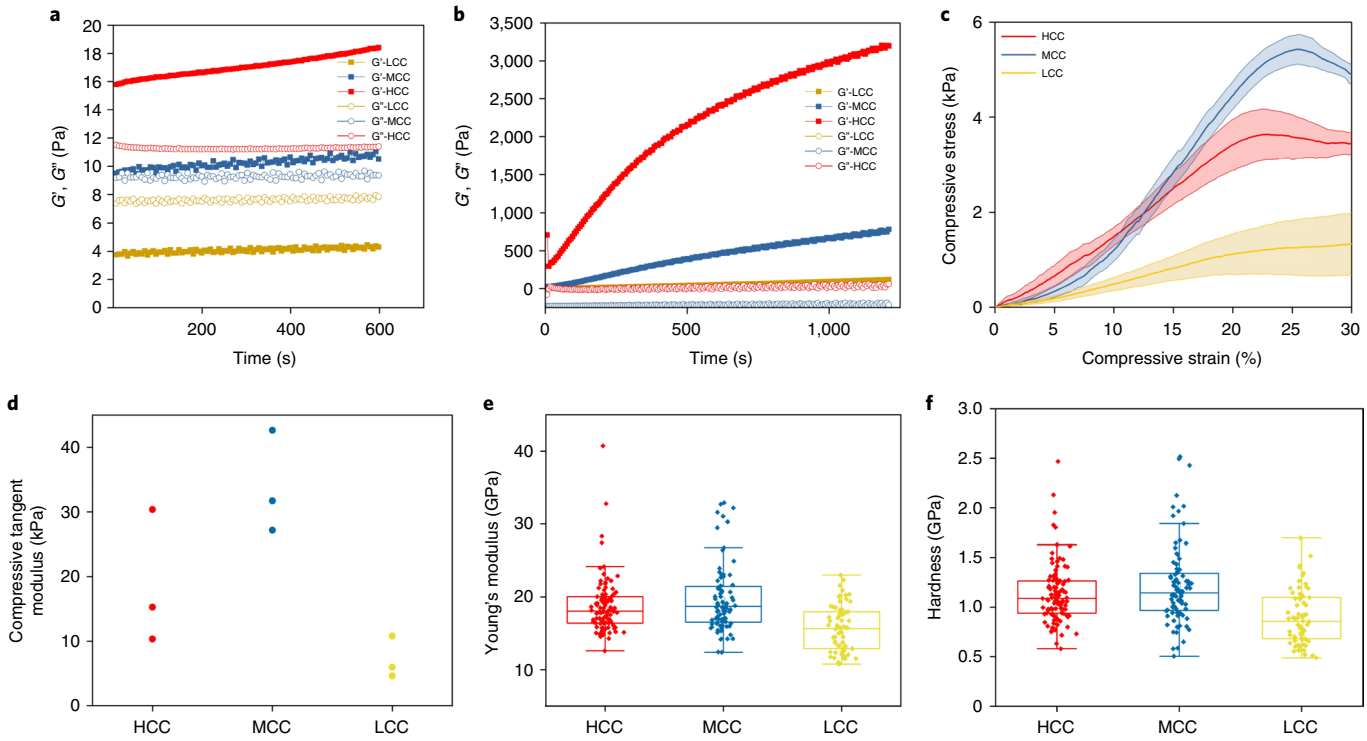

Fig. 2 | Mechanical characterization of P:C hydrogels. a, Storage (G') and loss modulus (G'') before NaOH addition. **b**, G' and G'' after NaOH addition (last step in hydrogel fabrication process). **c**, Unconfined compression of P:C post hydration for 12 h in 154 mM NaCl solution. Highlights around the curves correspond to the standard error of the mean. **d**, Calculated compressive tangent Young's moduli post hydration for 12 h in 154 mM NaCl solution. Difference in mean Young's moduli of MCC compared with LCC was statistically significant ($^*P < 0.05$). Points of the same colour represent replicates. **e**, Young's moduli on dry P:C hydrogels measured from nanoindentation studies. No significant statistical difference in Young's moduli of dried materials was observed. Respective HCC, MCC and LCC upper quartile: 20.0, 21.4 and 17.9; lower quartile: 16.4, 16.6 and 12.9; median: 18.1, 18.7 and 15.7; mean: 18.8, 19.8 and 15.7; min.: 12.6, 12.4 and 10.8; max.: 40.7, 32.9 and 23.0. **f**, Hardness of dry P:C 1:1 measured with nanoindentation. No significant statistical difference in the hardness of dried materials was observed. Respective HCC, MCC and LCC upper quartile: 1.26, 1.34 and 1.10; lower quartile: 0.94, 0.97 and 0.68; median: 1.09, 1.14 and 0.86; mean: 1.13, 1.22 and 0.90; min.: 0.58, 0.50 and 0.49; max.: 2.47, 2.52 and 1.70. Boxplots show the median (horizontal line), 25th and 75th percentiles (lower and upper boundaries, respectively). Whiskers extend to data points that lie within 1.5 times the interquartile ranges of the 25th and 75th quartiles, and observations that fall outside this range are displayed independently.

R. tropici CIAT 899 in the inoculum (N) by multiplying C_a with the volume (V) as shown in equation (1).

$$N = C_a \times V = C_a \times \left(\frac{4}{3}\pi ABC - \frac{4}{3}\pi abc\right) \quad (1)$$

where $A = a + t$, $B = b + t$ and $C = c + t$. Using $a = 0.25$ cm, $b = 0.25$ cm, $c = 0.5$ cm, $t = 0.0005$ cm and $C_a = 10^{10}$ cm^{-3}, then $N = 6.56 \times 10^6$ *R. tropici* CIAT 899 encapsulated per seed. The external layer (layer 2) is a mucilage-like mixture of pectin/carboxymethylcellulose (P:C, 1:1) that contains nutrients and upon sowing forms a hydrogel that acts as a water jacket and provides a suitable environment for rhizobia resuscitation and growth (Fig. 1a,b). Layer 2 was designed as a food gel[31] and contains Ca^{2+} ions that act as crosslinker for pectins' galacturonic acid residues, providing stability to the gel and yielding a gel content of around 65% (Fig. 1c). Carboxymethylcellulose (CMC) molecules present in layer 2 fill the gaps in the pectin network and confer water superabsorption properties and enhance water retention. In Supplementary Fig. 1, we report the investigation of P:C hydrogel volume variation in 154 mM NaCl solution due to water absorption and gel content (GC) as a function of relative pectin and CMC content and of increasing Ca^{2+} concentrations. Volume variation upon rehydration and GC of pectin, CMC and their mixtures indicated that a P:C of 1:1 provides the best performance as a trade-off between volume variation (indication of water uptake) and GC properties (indication of gel stability over time). The effects of biologically relevant Ca^{2+} concentrations (low, 5 mM, LCC; medium, 10 mM, MCC; high, 15 mM, HCC) in P:C gels were then investigated, given the strong beneficial effect of the dication on rhizobia symbiosis with leguminous plants[32]. P:C 1:1 volume increased in the first 3 h upon rehydration, decreased at the 6 h time point, recovered and plateaued at 12 h (Fig. 1e). The decrease in volume at 6 h was similar for all the materials considered and could be explained by the wash-off of non-crosslinked CMC molecules. Previously reported maximum swelling of pectin hydrogels crosslinked with glutaraldehyde matched the results obtained in this study[33], although the use of toxic crosslinkers should be avoided for agricultural applications. Further, studies of biodegradable hydrogels used to modify soil water-holding capacity have reported water absorption on the same order as layer 2[34]. Water retention is another important parameter to consider in semi-arid soils as the hydrogels can stabilize the humidity around seeds for extended periods of time, acting as a water buffer in-between watering periods[35]. The measurement of volume variation during air-drying indicated that all the P:C gels considered had similar water loss trends, but HCC and MCC gels retained water longer than LCC, given the higher initial volumes (Fig. 1f). The use of a different P:C ratio and lower concentrations of Ca^{2+} ions may further be used to regulate water retention (Supplementary Fig. 2). Water absorption studies for gels were also

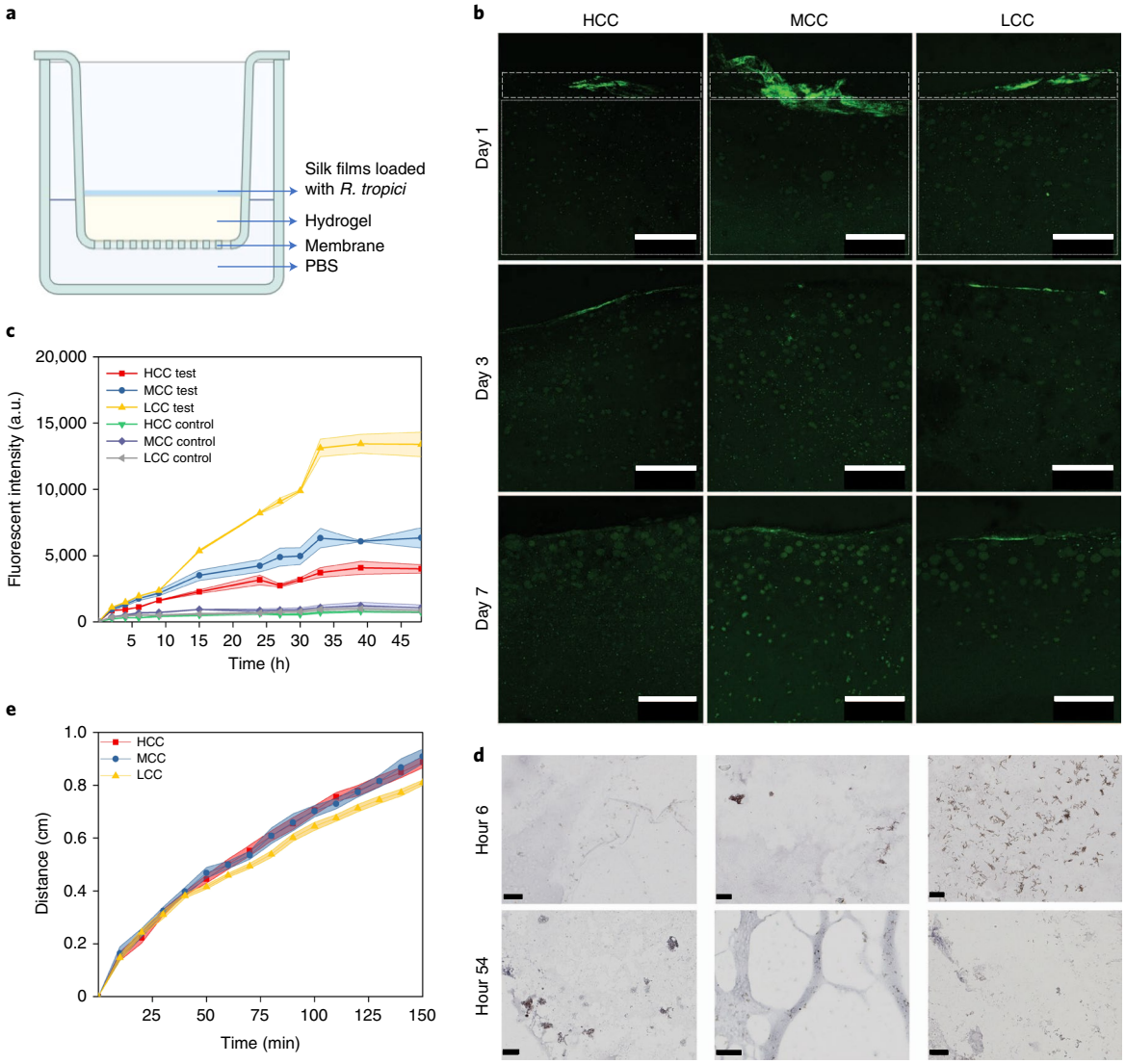

Fig. 3 | Use of P:C hydrogels as niche to grow *R. tropici* post rehydration. a, Experimental setup showing *R. tropici* CIAT 899 released from silk films, migrating and growing in P:C hydrogels simulating dry to swollen states. **b**, Representative confocal cross-section images showing microbe migration and growth in hydrogels, simulating post-sowing phenomena in soil. Dashed boxes highlight applied silk film location. Setup of experiment is shown in **a**. Scale bars, 500 µm. **c**, *R. tropici* CIAT 899-GFP expression in hydrated hydrogels, using the polysaccharides as the only energy source. Highlighted areas around curves correspond to the standard error of the mean. **d**, Representative histology sections of the hydrogels used as the only energy source, showing attraction of microbes to the hydrogels. Scale bars, 20 µm. **e**, Diffusion of fluorescein in hydrogels over time to model movement of nutrients/sugars.

conducted in soil to simulate how layer 2 would swell upon sowing. Volume variations of gels were measured after 24 h in three soil water content conditions (Fig. 1g). Gel volume significantly increased with soil water content ($P < 0.05$), but Ca^{2+} ions did not have a statistically significant effect on the swelling for the concentrations considered ($P > 0.05$). Interestingly, an order of magnitude was lost in P:C water uptake compared with swelling in saline solution, probably due to the lower water potential of soil and the compressive forces that soil applies on the gel and that limit swelling. However, even in semi-arid soils (soil water content, 10%), volume variation of around 250% indicated the capability of the coating to extract water from the environment and make it available to the rhizobacteria and the seed. A pressure of around 412 Pa is applied on the surface of a *P. vulgaris* seed (1.4 × 0.8 × 0.7 cm) sowed 3 cm below the surface of a semi-arid soil (average soil density (ρ_{avg}) ≅ 1.4 g cm^{-3}). Additionally, soil has a compression modulus of around 4–7 MPa (ref. [36]), indicating that the hydrogels may have complex interactions with the surrounding soil while reswelling occurs as a combination of soil deformation and expansion of air pockets present in the soil[37].

Mechanical properties and gel microstructure. Rheological measurements help to choose the required settings for material application onto seed surfaces. Rheological investigation of LCC, MCC and HCC solutions (that is, before gelling is triggered) showed a shear thinning behaviour (Supplementary Fig. 3) and the stability of the solutions' storage and loss modulus (G' and G'', respectively) (Fig. 2a) over time upon addition of Ca^{2+} ions into the P:C suspension. Exposure of P:C suspension to NaOH, causes a rapid increase in pH that results in immediate gelation of LCC, MCC and HCC. The rapid gelation hinders the application of the Winter–Chambon rule to calculate gelation time. Nonetheless, the evolution of G' and G'' post gelling was monitored over time (Fig. 2b) and showed an increase in G'' that was positively correlated with Ca^{2+} concentration. To further

evaluate the suitability of P:C gels to work as seed coating, we measured the mechanical properties of P:C 1:1 hydrogels through unconfined compression tests (Fig. 2c). MCC hydrogels displayed both the highest compressive strength (5.43 ± 0.31 kPa) (Fig. 2d) and Young's modulus (33.86 ± 4.60 kPa) (Fig. 2e). Nanoindentation tests were also conducted on dry P:C to determine their capability to sustain transportation and storage periods without being damaged. The measured Young's modulus (~15–20 GPa, Fig. 2e) and hardness (~1–1.5 GPa, Fig. 2f) were on the same order as currently available seed coatings[38]. Cross-sectional cryo-scanning electron microscopy was used to evaluate the microstructure of the hydrogels. Micrographs showed an interconnected microstructure with an assumed pore size of ~5 µm (Supplementary Fig. 4). However, the pore shape and dimension may have been affected by the formation of ice crystals during sample preparation, which is known to artificially increase the pore size, particularly in hydrogels with a weak structural integrity such as LCC[39].

Effectiveness to support rhizobacterial growth. To investigate the effectiveness of P:C hydrogels as niche to support *R. tropici* CIAT 899 resuscitation and growth, we designed two experimental setups. In the first study, *R. tropici* CIAT 899 were released from dissolving silk films into swelling P:C 1:1, as shown in Fig. 3a. In particular, we used *R. tropici* CIAT 899 harbouring a green fluorescent protein reporter (*R. tropici* CIAT 899-GFP) to use the fluorescent intensity signal over time as an indication of bacterial colonization and growth. After verifying that *R. tropici* CIAT 899-GFP could use seed mucilage as carbon source (using simulated basil mucilage as an example, Supplementary Fig. 5), we investigated the migration of *R. tropici* CIAT 899-GFP from silk film into P:C 1:1 formed at increasing concentrations of Ca^{2+} (Fig. 3a) and containing nutrients found in seed mucilage (that is, 20.9 mM D-(+)-xylose, 6.28 mM L-(+)-arabinose, 6.28 mM DL-arabinose, 8.94 mM L-rhamnose with a ratio of 30:9:9:14)[40].

The release of *R. tropici* CIAT 899-GFP from silk films and the subsequent P:C colonization was investigated using fluorescent microscopy (Fig. 3b)[41]. Silk films were dissolving gradually over time while green spots, corresponding to *R. tropici* CIAT 899-GFP microcolonies, were growing in size and numbers within the depth of the hydrogels. *R. tropici* CIAT 899-GFP microcolonies were more concentrated at the surface of the LCC and HCC gels on day 7, while *R. tropici* CIAT 899 -GFP colonization was more homogenously distributed in MCC samples. Interestingly, a size gradient could be observed in microcolonies present in MCC hydrogels, with larger colonies being visible closer to the source of *R. tropici* CIAT 899-GFP. To further investigate hydrogel colonization from the environment, we designed a second study where dry P:C 1:1 hydrogels were immersed in a solution containing *R. tropici* CIAT 899-GFP. GFP intensity in the hydrogels increased over time and plateaued at 32 h (Fig. 3c). GFP intensity was inversely proportional to the crosslinker content, that is, the lower the content of Ca^{2+} ions, the higher the GFP intensity. To determine the interplay between layer 2 swelling and bacterial colonization, we immersed dry P:C 1:1 in a 154 mM solution containing *R. tropici* CIAT 899-GFP (optical density measured at a wavelength of 600 nm (OD_{600}) ≈ 0.1). Histological sections at 6 h and 54 h post rehydration showed the presence of Gram-negative *R. tropici* CIAT 899-GFP within the gels (Fig. 3d and Supplementary Fig. 6), suggesting that layer 2 swelling may be able to recruit endogenous microorganisms present in the soil and further attract them post swelling due to the presence of nutrients in the hydrogel. To further support this assumption, diffusion of saccharides in the hydrogel was studied using fluorescein as a working model. Calculated diffusion coefficients were ~10^{-5} cm^2 s^{-1} and not influenced by the amount of crosslinks present in the hydrogels (that is, Ca^{2+} concentration during material fabrication) (Fig. 3e and Table 1)[42]. This result suggests that the rate of diffusion of nutrients was not the determining factor of *R. tropici* CIAT 899-GFP growth, but other features such as different pore sizes and geometries may have caused an increased colonization in MCC gels[43,44].

Table 1 | Calculated diffusion coefficients

Medium	Diffusion coefficient (fluorescein) (cm^2 s^{-1})
HCC	$3.32\times10^{-5}\pm8.83\times10^{-7}$
MCC	$4.00\times10^{-5}\pm1.31\times10^{-6}$
LCC	$3.96\times10^{-5}\pm1.38\times10^{-6}$
Water	4.20×10^{-6}

Coating biodegradation. The biodegradation of the seed coating was evaluated by exposing MCC hydrogels to soil. Biopolymer degradation in the absence of light is mostly catalysed by microbial activity through enzymatic degradation that accelerate proteolytic and carbohydrolytic processes. Important parameters such as type of indigenous microorganisms, temperature, soil type, composition, pH, salinity, water and carbon contents play prominent roles in determining how quickly biopolymers may be degraded. Figure 4a depicts the mass loss of MCC hydrogels over time when investigated at 16 °C in soil containing microorganisms. On days 14 and 28, almost 50 and 70% of the dry weight of the gel was lost. When exposed to soil containing sodium azide—a bacteriostat—the mass-loss rate of MCC decreased for the first 14 d compared with untreated soil, indicating the critical role of microorganisms in biopolymer degradation in soil. For longer time points (up to day 28), the mass loss increased and reached values similar to those measured for untreated soil, probably indicating the inefficacy of the sodium azide treatment in the long term. Biodegradation studies were also conducted in untreated soil at 25 °C and resulted in the complete biodegradation of LCC, MCC and HCC materials in less than 30 d (Supplementary Fig. 7). Biodegradation in sterilized soil only resulted in less than 50% of mass loss over a period of 30 d. The complete biodegradation of the coating within the life cycle of the plant is an important feature to minimize the environmental impact of agriculture and the release of pollutants into the soil. Recently, policymakers have promoted new laws that strictly regulate the biodegradation of polymers released in the environment for agricultural applications. For example, in January 2018 the European Chemicals Agency examined the need for a European Union-wide restriction on the use of intentionally added microplastic particles in products placed on the European Union market, including food and agricultural products, with non-biodegradable microplastics forecasted to be banned in 2025[45].

Seedling germination and growth in semi-arid conditions. All together, these results suggest that seed coating properties may be programmed by varying several parameters, including relative P:C concentration, amount of Ca^{2+} during materials fabrication and presence of nutrients to design an environment that can support resuscitation and growth of plant growth-promoting rhizobacteria. In particular, for the purpose of our study, we selected MCC as the hydrogel to conduct germination studies, given the combination of homogenous *R. tropici* CIAT 899 colonization, water absorption and mechanical properties. In a preliminary study, germination of *P. vulgaris* seeds was tested in a greenhouse setting by applying the following treatments: (1) no treatment (negative control); (2) inoculation with 3% polyvinylpyrrolidone solution with *R. tropici* CIAT 899-GFP (positive control); (3) bilayer seed coating with layer 2 applied via spray coating; and (4) bilayer coating with layer 2 applied via dip coating. Seedlings were checked for nodulation on

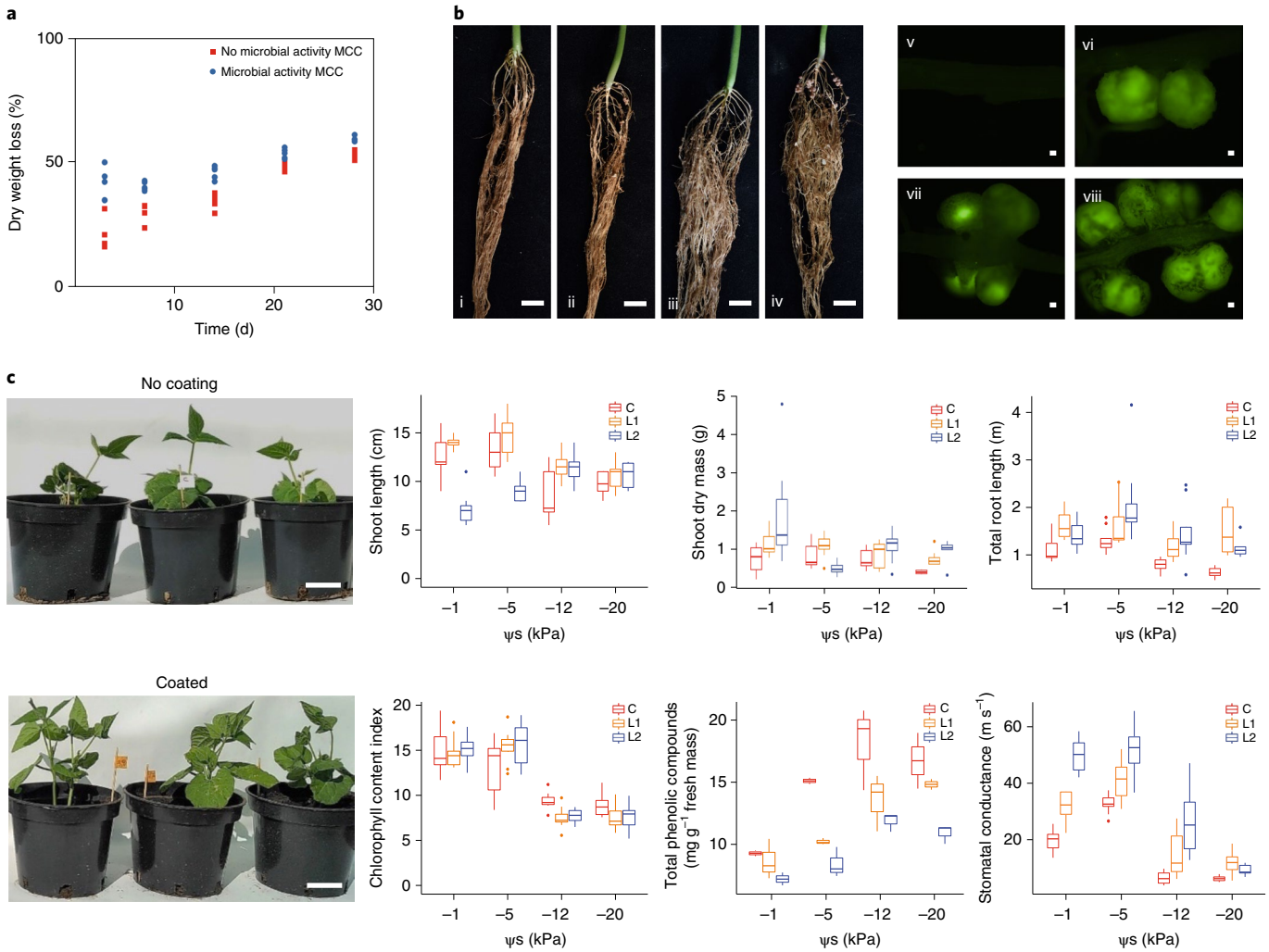

Fig. 4 | Degradation of seed coating material in soil and application to *P. vulgaris* to mitigate water stress. a, Degradation of P:C hydrogel with and without soil microbe activity in 25% soil moisture over a month at 16 °C. Dots correspond to collected data. **b**, Representative root images and corresponding fluorescent microscopy images of nodule formation for plants established from the following treatments: (i) and (v), no coating and no inoculation; (ii) and (vi), inoculation of *R. tropici* CIAT 899-GFP using a 3% polyvinylpyrrolidone solution; (iii) and (vii), bilayer coating with layer 2 applied via spray coating; and (iv) and (viii), bilayer coating with layer 2 applied via dip coating. Scale bars, 10 mm for root pictures and 100 μm for fluorescent microscope images. $N=18$ plants tested per treatment type with a 100% nodulation rate for seeds treated with *R. tropici* CIAT 899. No nodulation was visible on day 14 for the negative control. **c**, Growth of *P. vulgaris* at week 6 in water-stress regime from seeds that had no coating and those with L1 and L2 coatings. Scale bars, 10 cm. *P. vulgaris* establishment investigation is shown as a function of coating and water potential (Ψs) levels. Ψs = −1 kPa and −5 kPa correspond to healthy soil moisture content. Ψs = −12 kPa and −20 kPa represent mild and severe water-stress conditions, respectively. *P. vulgaris* plant establishment was investigated by measuring shoot length, shoot dry mass, total root length, chlorophyll content, total phenolic compounds and stomatal conductance. Boxplots show the median (horizontal line), 25th and 75th percentiles (lower and upper boundaries, respectively). Whiskers extend to data points that lie within 1.5 times the interquartile ranges of the 25th and 75th quartiles, and observations that fall outside this range are displayed independently.

day 14 after germination to ensure successful delivery of rhizobacteria and root colonization (Fig. 4b). A 100% nodulation rate was observed for all three procedures where *R. tropici* CIAT 899 were added to the soil. Application of layer 2 via both spray coating and dip coating resulted in roots that were more developed compared with the positive control, suggesting that the seed enhancement technology outperforms current standard materials and can be applied with tools largely available to growers.

To further test the efficacy of the two-layer coatings (L2) in mitigating environmental stressors typical of semi-arid regions, we conducted germination studies at the UM6P experimental farm in Ben Guerir, Morocco, using native soil (Fig. 4c). Soil analysis revealed a composition typical of sandy soils, that is, slightly alkaline and prone to induce drought stress due to limited water-retention capacity. The soil was rich in nitrogen and phosphate and concentrations of oligoelements such as manganese and zinc were sufficient, while there was a slight deficiency in copper content (Supplementary Table 1). To investigate the effectiveness of L2 in inducing water-stress tolerance, we exposed L2-coated *P. vulgaris* seeds to soils with decreasing water potential (Ψs), by altering the watering conditions to induce water-stress regimes (Fig. 4c). Seeds with no coating (C) and seeds coated only with layer 1 (L1) were used as control and one-way analysis of variance (ANOVA) with Bonferroni's correction was used to analyse the data collected. When comparing the different watering conditions in 150 g of soil per plant, it was observed that for mild (Ψs = −12 kPa) and severe (Ψs = −20 kPa) water-stress conditions, L2 coating statistically significantly influenced germination and plant health compared with the two controls.

L2 seeds resulted in higher shoot dry mass compared with C and L1 seeds for Ψs of −1, −12 and −20 kPa. Shoot length was not a factor that seemed to be determined by coating maybe because this was early on in the growth process. No statistically significant difference was found for shoot length between L2, L1 and C seeds for Ψs = −20 kPa. It was also observed that root architecture was significantly affected by seed and water treatments. Seeds germinated in soil with Ψs = −1 and −5 kPa had the longest roots compared with seeds germinated in water-stress conditions of Ψs = −12 and −20 kPa. Under water-stress regimes, roots from L2 and L1 seeds were statistically significantly longer compared with those from C seeds, indicating that the coating treatments provided a better environment for early root establishment. Measurement of chlorophyll content in leaves showed that watering regime but not seed coating affected the production of the green pigment. The amount of total phenolic compounds is correlated with drought stress as plants release phenolic compounds to mitigate water deficit[46]. Total phenolic compounds was statistically significantly lower for L2 seeds compared with L1 and C seeds, indicating the contribution of the designed hydrogel to induce water-stress tolerance. Measurement of stomatal conductance corroborated this finding. *P. vulgaris* cultured in water-stress regimes showed lower stomatal conductance to limit water loss[47]. In our experiments, L2 seeds showed statistically significantly higher stomatal conductance for Ψs = −1, −5 and −12 kPa compared with the L1 and C seeds and a higher stomatal conductance compared with C seeds for Ψs = −20 kPa, indicating a better tolerance to water deficiency. All together, these results indicate that the L2 coating positively influence plant establishment of *P. vulgaris* in a semi-arid soil and under water stress.

Discussion

In this study, we investigated the use of a biomaterials and drug delivery approach to engineer a programmable seed coating technology for effective delivery and growth of rhizobacteria in the spermosphere. Activated upon sowing, the two-layered coating technology enabled the resuscitation and self-replication of rhizobia within a biopolymer-based hydrogel that resembles seed mucilage and resulted in the formation of microbial colonies that formed symbiotic nodules with plant roots and induced water-stress tolerance in semi-arid conditions. Furthermore, the use of biopolymers generally used in food gels provide a largely available, cost-effective and non-toxic solution to mitigate abiotic stress. Together, these findings open the door to the use of enhanced seed coating technologies to address specific weather and soil conditions, to adapt agriculture to changes in climate patterns while also minimizing the use of scarce and energy-intensive inputs. Future studies will focus on the beneficial role of rhizobacteria preserved and delivered using the coating technology described in this work, highlighting their role in improving plant growth and soil health, and mitigating environmental impact.

Methods

Materials. Materials fabrication, hydration and dehydration studies are reported below. Extensive details of the experimental procedures are reported in Supplementary Information.

Hydrogel fabrication. Four types of gel were prepared with different ratios of low-methoxylated pectin (P) (from citrus peel, >74% galacturonic acid, >6.7% methoxy groups; Sigma-Aldrich) to NaCMC (C) (molecular weight 90,000 g mol^{-1}, degree of substitution 0.7; Sigma-Aldrich). The tested P:C ratios were 1:0, 3:1, 1:1, and 1:3, but the total amount of polysaccharides was 5 wt% for all solutions. For the gel preparation, monomeric sugars (D-(+)-xylose, 20.9 mM; L-(+)-arabinose, 6.28 mM; DL-arabinose, 6.28 mM; L-rhamnose, 8.94 mM; Sigma-Aldrich; with the ratio 30:9:9:14) were first added to deionized (DI) water to mimic the ratio found in basil seeds[40]. After complete mixing of the polysaccharides in the sugar solution, three calcium chloride ($CaCl_2$, Sigma-Aldrich) concentrations were added to each mixture from a 1 mM $CaCl_2$ stock solution in DI water: HCC (15 mM), MCC (10 mM) and LCC (5 mM). After leaving the solution for 24 h, 70 mol% (mol percentage of polysaccharides) of OH^- (from 2 M NaOH stock solution) was added to each gel to increase the pH and lead to gelation, according to the egg-box model. After 48 h, the samples were prepared and air-dried for 24 h at r.t. From these gels, the best P:C ratio was selected by analysing both the water content over time and the GC. Only materials with the selected P:C ratio were then optimized (for pH and $CaCl_2$ concentrations). Indeed, because the pH is only important for pectin gelation and not for NaCMC, the added NaOH amount had to be adjusted: 70 mol% of galacturonic acid (pectin's principal monomer) rather than 70 mol% of all polysaccharides. $CaCl_2$ concentrations subsequently needed to be increased for the mechanical integrity of the gel. Finally, full characterization was only done for the materials with the selected P:C ratio.

Mechanical properties. To evaluate the strength of wet samples, non-confined compression tests were conducted (5943 Instron) on round gel samples ($n = 3$, diameter 38 mm, thickness 16 mm). The strain speed rate was set to 100% min^{-1}, and the whole experiment was filmed until a strain compression of 30%. Tangents to all compressive stress–strain curves were calculated at 5, 10 and 15% strain to evaluate which tangents were fitting the best linear (elastic) regions of each gel type.

Nanoindentation. Nanoindentaion measurements were performed on a Hysitron TriboIndenter with a nanoDMA transducer (Bruker). Samples were indented in load control mode with a peak force of 500 μN and a standard load-peak hold-unload function. Reduced modulus was calculated by fitting the unloading data (with upper and lower limits being 95% and 20%, respectively) using the Oliver–Pharr method and converted to Young's modulus assuming a Poisson's ratio of 0.33 for all samples. Each type of sample was prepared and indented in triplets to ensure good fabrication repeatability. For each sample, indentation was performed at 3 locations for a total of 36 points (6 × 6 grid with an increment of 20 μm in both directions) at each location to ensure statistical reliability of the modulus measurements.

Bacterial growth. To assess bacterial growth in the presence of the selected hydrogels, two experiments were conducted. For both experiments, growth media were prepared by mixing 5 g Bacto Peptone (BD Biosciences), 3 g yeast extract (Sigma-Aldrich) and 10 ml 0.7 M $CaCl_2$ solution with 1 litre DI water. The following antibiotics (Sigma-Aldrich) were then added: rifampicin (25 mg ml^{-1}), nalidixic acid (20 mg ml^{-1}) and tetracycline (10 mg ml^{-1}). The media was sterilized by autoclaving for 50 min at 120 °C. *R. tropici* CIAT 899 was grown in media overnight (28 °C, 250 r.p.m.) in 14 ml falcon round-bottom tubes (Corning). The tubes were then centrifuged at 3,850 × *g* for 10 min (5910 R, Eppendorf) and the bacterial pellets were resuspended in 5 ml PBS (BupHTM phosphate-buffered saline packs, ThermoFisher Scientific). The OD_{600} was finally adjusted to 0.1 before the following two experiments were performed.

Experiment 1. Two MCC gels were fabricated, one with the usual basil-inspired monosaccharides and the other with the same amount of sucrose instead. Because it is known that *R. tropici* CIAT 899 can digest sucrose, this experiment would thus give information about the bacterial digestion of basil sugars. Forty-eight hours after the NaOH addition, 12 square hydrogel samples (1 cm^3) were cut out and air-dried for 24 h at r.t. The gels were then rehydrated in PBS for 12 h in 15 ml tubes. For controls ($n = 3$), the PBS was renewed, and for positive samples ($n = 3$), the initial PBS was replaced by PBS with *R. tropici* CIAT 899 ($OD_{600} = 0.1$). *R. tropici* CIAT 899 synthesizing green fluorescent protein (*R. tropici* CIAT 899-GFP)[41] were used to conduct hydrogel colonization studies. GFP fluorescence intensity of the solution was repeatedly measured at the following time points: 5, 8, 24, 30, 36 and 48 h (Safire2). The excitation light was 491 nm, the emission light was 530 nm, and the gain was set to 70. GFP fluorescent intensity gave information on the amount of the fluorescent reporter expressed by *R. tropici* CIAT 899-GFP and it was used as an indication of living bacteria and their growth.

Experiment 2. The fluorescence experiment was repeated with the three P:C 1:1 gels (LCC, MCC and HCC). The time points at which fluorescence was repeatedly measured were 2, 4, 6, 9, 15, 24, 27, 30, 33, 39 and 48 h.

Histological sections. To determine whether bacteria were attracted by the hydrogel and migrated inside them, pieces of hydrogels were retrieved after 6 and 54 h of incubation with *R. tropici* CIAT 899-GFP, fixed in 10% formalin (Sigma-Aldrich) for 18 h, washed twice with PBS, and casted into HistoGel (ThermoFisher Scientific). Distinct samples were used for each time point considered. After 30 min, two slices were cut out from the sample and placed in a cassette in formalin for an additional hour. Finally, all gels were conserved in 70% ethanol before being brought for histology (Gram-negative staining, Hope Babette Tang Histology Facility, Koch Institute, MIT, MA).

Migration studies. An aqueous solution of silk fibroin (1% (w/v), boiled for 45 min) was prepared from silkworm cocoons (Tajima Shoji) as described in Rockwood et al.[20] and mixed with a 1% (w/v) aqueous solution of trehalose (D-(+)-trehalose anhydrous, TCI Chemicals). The two solutions were added together to a final silk/trehalose ratio of 1:3. *R. tropici* CIAT 899-GFP were centrifuged at 3,850 × *g* for 10 min (Eppendorf 5910 R) and the pellet was resuspended in the silk/trehalose solution until an OD_{600} of 0.1 was reached. Fifty millilitres of this solution was

drop-casted on a PDMS sheet and air-dried for 48 h at r.t. to form a film. In the meantime, the three P:C 1:1 gels were prepared as explained earlier. Right after the addition of NaOH, each viscous solution was transferred to the inserts of a 12-transwell plate (Corning) ($n=4$) to reach a height of 2 mm. The gels were finally air-dried for 48 h at r.t. On top of the dried gel, a dry film was deposited on day 0. At the bottom of the transwell plate, PBS was added so that only the bottom of the gel touched the solution through the permeable membrane. One sample of each gel was taken out on days 1, 3 and 7, that is, distinct samples were used for each time point considered. The samples were fixed with 10% formalin solution for 30 min (Sigma-Aldrich) and incubated with the TrueVIEW kit (Vector Laboratories) for 5 min to quench the autofluorescence of the hydrogels. A cross-section of each gel was then imaged with a confocal microscope (inverted Ti Nikon1AR ultra-fast spectral scanning confocal microscope) at each time point to observe the migration of the microbes across the hydrogel. All images were taken with exactly the same parameters. The fluorescent images were then processed with the ImageJ software to obtain a maximum intensity Z-projection.

Diffusion studies. To compare the diffusion of nutrients through hydrogels, 4 ml solutions of LCC, MCC and HCC hydrogel were prepared and added to 5 ml tubes and solidified for 48 h. Gels were then hydrated in 154 mM NaCl solution for 24 h before the diffusion study. One millilitre of a solution of fluorescein (100 mM) in water was pipetted on top of each hydrogel and the gels were photographed every 10 min for 150 min. The distance the fluorophore had travelled was measured at each time point and these data were used to calculate the diffusion rate of small molecules through the hydrogel[42]. Samples were measured repeatedly at the time points considered.

Material biodegradation. Degradation of hydrogels in soil was evaluated over a one-month period. Dry samples of each gel (five 8 mm punches, $n=3$) were weighed beforehand (W_i). The samples in 100-mm-mesh tea bags were buried in 25% hydrated soil. Fifty-millilitre silk films containing *R. tropici* CIAT 899 ($OD_{600}=0.1$) were prepared as explained above and one film was added to each tea bag. The moisture condition of the soil was monitored with a hydrometer and DI water was added when needed to maintain the 25% moisture level (5 ml every 3 d). A sample of each gel was taken out on days 1, 3, 7, 14 and 28 (measurements were then taken from distinct samples). Samples were quickly washed in 154 mM NaCl solution and then air-dried for 24 h at r.t. before their weight was measured (W_d). Degraded gel (DG) amount was calculated as described in equation (2):

$$\mathrm{DG} = \frac{W_i - W_d}{W_i} 100 \quad (2)$$

where W_i is the initial dry weight of the sample and W_d is the dry weight of the samples after some time in PBS and bacteria or in soil, depending on the experiment. To investigate the effects of a reduced microbial activity on the material biodegradation, 2% sodium azide solution was mixed with the soil (1 ml per gram of soil)[48]. Biodegradation studies were conducted at 16 and 24 °C.

Rheology. Isothermal gelation studies were conducted with a TA Instruments stress-controlled AR-G2 rheometer with a 40 mm, 2∞ cone-and-plate fixture at 25 °C. NaOH was added to the polymer mixture to induce bond formation (time $t=0$), the mixture was then immediately transferred onto just the rheometer plate, and measurement started at $t=60$–90 s. For time sweeping tests, storage moduli G' and loss moduli G'' were monitored as a function of time at a 1 Hz frequency and a 2% stress strain under constant temperature (25 °C).

Fluorescence calibration. To convert all fluorescence intensity numbers to OD_{600} values, a calibration curve was made. *R. tropici* CIAT 899 were diluted in PBS at seven different OD_{600}: 0, 0.1, 0.3, 0.5, 0.7, 1 and 1.1. The corresponding fluorescence intensities were measured and plotted against the OD_{600}. The excitation light was 491 nm, the emission light was 530 nm, and the gain was set to 70. A linear model was fitted with MATLAB (R2018a, MathWorks).

Statistical analysis. Statistical analysis was performed with MATLAB (R2018a, MathWorks). Normality of the data was verified using the Jarque–Bera test. A one-way ANOVA was applied, followed by pairwise comparison if the results showed a statistically significant difference between the groups ($P<0.05$). Bonferroni's correction was applied to counter the effects of multiple comparisons.

Seed coating. P. vulgaris seeds were surface-sterilized with 10% bleach for 3 min, rinsed in H_2O three times and left to air dry. Eighty millilitres of *R. tropici* CIAT 899-GFP ($OD_{600}=1$) was centrifuged at 3,850 × *g* in an Eppendorf centrifuge 5910 R. The supernatant was discarded and 8 ml of dry 6 wt% silk fibroin/trehalose (1:3) solution was added to the spun-down *R. tropici* CIAT 899-GFP. Air-dried seeds were then dipped into this solution for 120 s, taken out and left to dry (layer 1). After slightly drying, the seeds were either dip-coated into a hydrogel gelation solution just after adding NaOH and left to dry (layer 2 dip) or slightly sprayed with the hydrogel solution (layer 2 spray). After drying, the seeds were planted at the 24 h mark.

Growth conditions. Initial assessment of seed growth and nodulation was carried out in African violet soil. Germination of *P. vulgaris* seeds was tested in a greenhouse setting by applying the following treatments: (1) no treatment (negative control); (2) inoculation with 3% polyvinylpyrrolidone solution with *R. tropici* CIAT 899-GFP (positive control); (3) bilayer seed coating with layer 2 applied via spray coating; and (4) bilayer coating with layer 2 applied via dip coating[49,50]. Seedlings were checked for nodulation on day 14 after germination to ensure successful delivery of rhizobacteria and root colonization. $N=18$ seeds per treatment were used. Additionally, no statistically significant changes in soil electrical conductivity (EC) were measured in soil where coated and uncoated seeds have germinated (2.13 ± 0.03 and 2.12 ± 0.02 mS cm^{-1}, respectively), indicating that the ions present in the coating do not significantly affect EC.

Following this preliminary assessment, seed growth was carried out in semi-arid soil at UM6P experimental farm in Ben Guerir, Morocco. Watering conditions were adjusted to obtain soils with an average water potential (Ψs) of −1, −5, −12 and −20 kPa over a 48 h time interval. Mild and severe water-stress growth conditions corresponded to $\Psi s=-12$ and −20 kPa, respectively. Soil tensiometers were made from a ceramic cup connected to an acrylic glass tube and had a 136PC15G1 bridge pressure sensor (Micro Switch) on the top to measure the pressure inside the tubing caused by water dynamics between the soil and water-filled tube. Tensiometers were used for each treatment in three replicates to monitor the water potential. Water lost through evapotranspiration was replenished to maintain the desired water potential. Healthy seeds from each treatment were evenly germinated on 10 cm plastic trays containing 150 g of a substrate mixture composed of 30% sieved sand (2 mm) and topsoil, manually shifted from stone. After adding water treatment solution to each replicate, trays were placed in the growth chamber with relative humidity of 65 to 70%, night temperature of 16 °C, day temperature of 24 °C and photoperiod of 16/8 h. All the treatments were laid out in a completely randomized design, replicated five times, and kept for recording physiological attributes. To ascertain the role of seed coating in alleviating drought stress and to evaluate its effect on plant establishment and behaviour during the growth cycle, three random seedlings were transplanted to large pots (30 cm deep, 20 cm diameter) 20 d after sowing. Pots containing 4 kg of the substrate mixture were kept under the greenhouse to allow root and leaf development. Irrigation was applied following the same water treatments used earlier. Different measurements from distinct samples were taken to investigate the treatment general effects: (1) shoot length over time; (2) shoot dry weight; (3) total root length (that is, total sum of the length of the roots) measured with WinRhizo (Regent Instruments) root scanner; (4) stomatal conductance, measured using an SC-1 leaf porometer (Decagon Devices); (5) chlorophyll content, measured with a CL-01 chlorophyll content system (Hansatech Instruments); and (6) total phenolic compounds, measured by grinding fragments of leaves and roots (0.5 g of fresh mass) in a mortar containing 5 ml of 50% ethanol solution. The extracts were collected in tubes with lids and labelled, then left in the refrigerator overnight. Upon adding 0.5 ml chloroform to 3 ml of extract, tubes were vortexed and centrifuged for 5 min at 7,100 × *g*. Total phenolic compounds assay was performed using the Folin–Ciocalteu reagent. Briefly, 0.5 ml extract, 3 ml distilled water and 0.5 ml Na_2CO_3 (20%) were mixed in a test tube. After 3 min, 0.5 ml Folin–Ciocalteu reagent was added. The test tubes were left for 30 min at 40 °C before measuring absorbance at 760 nm. The content of phenolic compounds was calculated using gallic acid for the standard curve and expressed in milligrams per gram of fresh leaf matter.

Reporting Summary. Further information on research design is available in the Nature Research Reporting Summary linked to this article.

Data availability

All relevant data are included in the article, Supplementary Information and in the Source Data files. All the other raw data are available from the authors upon request. Source data are provided with this paper.

Received: 23 November 2020; Accepted: 3 June 2021;
Published online: 8 July 2021

References

1. *Status of the World's Soil Resources* (FAO, 2015).
2. Ricciardi, V. et al. A scoping review of research funding for small-scale farmers in water scarce regions. *Nat. Sustain.* **3**, 836–844 (2020).
3. *The State of Food Security and Nutrition in the World 2019* (FAO, IFAD, UNICEF, WFP and WHO, 2019).
4. Behera, S. & Mahanwar, P. A. Superabsorbent polymers in agriculture and other applications: a review. *Polym. Technol. Mater.* **59**, 341–356 (2020).
5. Stahl, J. D., Cameron, M. D., Haselbach, J. & Aust, S. D. Biodegradation of superabsorbent polymers in soil. *Environ. Sci. Pollut. Res.* **7**, 83–88 (2000).
6. Niu, X., Song, L., Xiao, Y. & Ge, W. Drought-tolerant plant growth-promoting rhizobacteria associated with foxtail millet in a semi-arid agroecosystem and their potential in alleviating drought stress. *Front. Microbiol.* **8**, 2580 (2018).
7. Kuypers, M. M. M., Marchant, H. K. & Kartal, B. The microbial nitrogen-cycling network. *Nat. Rev. Microbiol.* **16**, 263–276 (2018).

8. Enebe, M. C. & Babalola, O. O. The influence of plant growth-promoting rhizobacteria in plant tolerance to abiotic stress: a survival strategy. *Appl. Microbiol. Biotechnol.* **102**, 7821–7835 (2018).
9. Soumare, A. et al. Exploiting biological nitrogen fixation: a route towards a sustainable agriculture. *Plants* **9**, 1011 (2020).
10. McIntyre, H. J. et al. Trehalose biosynthesis in *Rhizobium leguminosarum* bv. *trifolii* and its role in desiccation tolerance. *Appl. Environ. Microbiol.* **73**, 3984–3992 (2007).
11. Vriezen, J. A., de Bruijn, F. J. & Nüsslein, K. R. Desiccation induces viable but non-culturable cells in *Sinorhizobium meliloti* 1021. *AMB Express* **2**, 6 (2012).
12. Geetha, S. J. & Joshi, S. J. Engineering rhizobial bioinoculants: a strategy to improve iron nutrition. *Sci. World J.* https://doi.org/10.1155/2013/315890 (2013).
13. Molina-Romero, D. et al. Compatible bacterial mixture, tolerant to desiccation, improves maize plant growth. *PLoS ONE* **12**, e0187913 (2017).
14. Teixeira, A., Iannetta, P., Binnie, K., Valentine, T. A. & Toorop, P. Myxospermous seed-mucilage quantity correlates with environmental gradients indicative of water-deficit stress: *Plantago* species as a model. *Plant Soil* **446**, 343–356 (2020).
15. Western, T. L. The sticky tale of seed coat mucilages: production, genetics and role in seed germination and dispersal. *Seed Sci. Res.* **22**, 1–25 (2012).
16. Kreitschitz, A. & Gorb, S. N. The micro- and nanoscale spatial architecture of the seed mucilage–comparative study of selected plant species. *PLoS ONE* **13**, e0200522 (2018).
17. Phan, J. L. & Burton, R. A. New insights into the composition and structure of seed mucilage. *Annu. Plant Rev. Online* https://doi.org/10.1002/9781119312994.apr0606 (2018).
18. Sun, H. & Marelli, B. Growing silk fibroin in advanced materials for food security. *MRS Commun.* https://doi.org/10.1557/s43579-020-00003-x (2021).
19. Zhou, Z. et al. Engineering the future of silk materials through advanced manufacturing. *Adv. Mater.* **30**, 1706983 (2018).
20. Rockwood, D. N. et al. Materials fabrication from *Bombyx mori* silk fibroin. *Nat. Protoc.* **6**, 1612–1631 (2011).
21. Marelli, B., Brenckle, M. A., Kaplan, D. L. & Omenetto, F. G. Silk fibroin as edible coating for perishable food preservation. *Sci. Rep.* **6**, 25263 (2016).
22. Marelli, B. et al. Programming function into mechanical forms by directed assembly of silk bulk materials. *Proc. Natl Acad. Sci. USA* **114**, 451–456 (2017).
23. Kim, D. et al. A microneedle technology for sampling and sensing bacteria in the food supply chain. *Adv. Funct. Mater.* **31**, 2005370 (2021).
24. Cao, Y., Lim, E., Xu, M., Weng, J. K. & Marelli, B. Precision delivery of multiscale payloads to tissue-specific targets in plants. *Adv. Sci.* **7**, 1903551 (2020).
25. Sun, H. & Marelli, B. Polypeptide templating for designer hierarchical materials. *Nat. Commun.* **11**, 351 (2020).
26. Pritchard, E. M. & Kaplan, D. L. Silk fibroin biomaterials for controlled release drug delivery. *Expert Opin. Drug Deliv.* **8**, 797–811 (2011).
27. Crowe, J. H., Carpenter, J. F. & Crowe, L. M. The role of vitrification in anhydrobiosis. *Annu. Rev. Physiol.* **60**, 73–103 (1998).
28. Boothby, T. C. et al. Tardigrades use intrinsically disordered proteins to survive desiccation. *Mol. Cell* **65**, 975–984.e5 (2017).
29. Zvinavashe, A. T., Lim, E., Sun, H. & Marelli, B. A bioinspired approach to engineer seed microenvironment to boost germination and mitigate soil salinity. *Proc. Natl Acad. Sci. USA* **116**, 25555–25561 (2019).
30. Vílchez, S., Tunnacliffe, A. & Manzanera, M. Tolerance of plastic-encapsulated *Pseudomonas putida* KT2440 to chemical stress. *Extremophiles* **12**, 297–299 (2008).
31. Cao, Y. & Mezzenga, R. Design principles of food gels. *Nat. Food* **1**, 106–118 (2020).
32. Redondo-Nieto, M., Wilmot, A. R., El-Hamdaoui, A., Bonilla, I. & Bolaños, L. Relationship between boron and calcium in the N_2-fixing legume–rhizobia symbiosis. *Plant. Cell Environ.* **26**, 1905–1915 (2003).
33. Yoshimura, T., Sengoku, K. & Fujioka, R. Pectin-based superabsorbent hydrogels crosslinked by some chemicals: synthesis and characterization. *Polym. Bull.* **55**, 123–129 (2005).
34. Pathak, V. & Ambrose, R. P. K. Starch-based biodegradable hydrogel as seed coating for corn to improve early growth under water shortage. *J. Appl. Polym. Sci.* **137**, 48523 (2020).
35. Ahn, S. & Lee, S. J. Nano/micro natural patterns of hydrogels against water loss. *ACS Appl. Bio Mater.* **3**, 1293–1304 (2020).
36. Bakholdin, B. V. & Chashchikhina, L. P. Determination of the compression modulus of soils from compression-test data for calculation of pile-foundation settlements. *Soil Mech. Found. Eng.* **36**, 9–12 (1999).
37. Nataraj, M. S. & McManis, K. L. Strength and deformation properties of soils reinforced with fibrillated fibers. *Geosynth. Int.* **4**, 65–79 (1997).
38. Taylor, A. G. et al. Seed enhancements. *Seed Sci. Res.* **8**, 245–256 (1998).
39. Li, J. & Mooney, D. J. Designing hydrogels for controlled drug delivery. *Nat. Rev. Mater.* **1**, 16071 (2016).
40. Samateh, M. et al. Unravelling the secret of seed-based gels in water: the nanoscale 3D network formation. *Sci. Rep.* **8**, 7315 (2018).
41. Nanjareddy, K. et al. Nitrate regulates rhizobial and mycorrhizal symbiosis in common bean (*Phaseolus vulgaris* L.). *J. Integr. Plant Biol.* **56**, 281–298 (2014).
42. Yin, N. et al. Bacterial cellulose as a substrate for microbial cell culture. *Appl. Environ. Microbiol.* **80**, 1926–1932 (2014).
43. Kandemir, N., Vollmer, W., Jakubovics, N. S. & Chen, J. Mechanical interactions between bacteria and hydrogels. *Sci. Rep.* **8**, 10893 (2018).
44. Lichter, J. A. et al. Substrata mechanical stiffness can regulate adhesion of viable bacteria. *Biomacromolecules* **9**, 1571–1578 (2008).
45. *Restricting the Use of Intentionally Added Microplastic Particles to Consumer or Professional Use Products of Any Kind* Annex XV Restriction Report (ECHA, 2019).
46. Mansori, M. et al. Seaweed extract effect on water deficit and antioxidative mechanisms in bean plants (*Phaseolus vulgaris* L.). *J. Appl. Phycol.* **27**, 1689–1698 (2015).
47. Beebe, S. E., Rao, I. M., Blair, M. W. & Acosta-Gallegos, J. A. Phenotyping common beans for adaptation to drought. *Front. Physiol.* **4**, 35 (2013).
48. Trevors, J. T. Sterilisation and inhibition of microbial activity in soil. *J. Microbiol. Methods* **26**, 53–59 (1996).
49. Deaker, R., Roughley, R. J. & Kennedy, I. R. Legume seed inoculation technology—a review. *Soil Biol. Biochem.* **36**, 1275–1288 (2004).
50. Mukhtar, S., Shahid, I., Mehnaz, S. & Malik, K. A. Assessment of two carrier materials for phosphate solubilising biofertilizers and their effect on growth of wheat (*Triticum aestivum* L.). *Microbiol. Res.* **205**, 107–117 (2017).

Acknowledgements

We acknowledge M. Lara for *R. tropici* CIAT 899-GFP from Universidad Nacional Autonoma de Mexico, OCP S.A. and the Université Mohammed VI Polytechnique–MIT Research Program. This work was partially supported by the Office of Naval Research (Award No. N000141812258), the National Science Foundation (Award No. CMMI-1752172) and the MIT Paul M. Cook Career Development Professorship. Schematics in Fig. 1a,b were created with BioRender.com.

Author contributions

A.T.Z., J.L., M.M., B.M. and L.K. designed the study. A.T.Z., J.L., M.M., H.S., S.M., D.K. and H.M.E.F. collected and analysed the data. All authors contributed to the discussion and interpretation of the results. The manuscript was drafted by A.T.Z., J.L., H.S., M.M, L.K and B.M. and reviewed and approved by the other authors.

Competing interests

B.M. and A.T.Z. are co-inventors in a patent application (US Patent application no. 63/036,088) that describes the coating technology reported in this study. B.M. is co-founder of Mori, Inc., a company that develops silk-based edible coatings to extend the shelf life of food. All other authors have no competing interests.

Additional information

Supplementary information The online version contains supplementary material available at https://doi.org/10.1038/s43016-021-00315-8.

Correspondence and requests for materials should be addressed to B.M.

Peer review information *Nature Food* thanks David Britt, Haihua Xiao and Maximino Manzanera for their contribution to the peer review of this work.

Reprints and permissions information is available at www.nature.com/reprints.

Publisher's note Springer Nature remains neutral with regard to jurisdictional claims in published maps and institutional affiliations.

nature research

Corresponding author(s): Benedetto Marelli

Last updated by author(s): May 21, 2021

Reporting Summary

Nature Research wishes to improve the reproducibility of the work that we publish. This form provides structure for consistency and transparency in reporting. For further information on Nature Research policies, see our Editorial Policies and the Editorial Policy Checklist.

Statistics

For all statistical analyses, confirm that the following items are present in the figure legend, table legend, main text, or Methods section.

n/a	Confirmed	
☐	☒	The exact sample size (*n*) for each experimental group/condition, given as a discrete number and unit of measurement
☐	☒	A statement on whether measurements were taken from distinct samples or whether the same sample was measured repeatedly
☐	☒	The statistical test(s) used AND whether they are one- or two-sided *Only common tests should be described solely by name; describe more complex techniques in the Methods section.*
☒	☐	A description of all covariates tested
☒	☐	A description of any assumptions or corrections, such as tests of normality and adjustment for multiple comparisons
☐	☒	A full description of the statistical parameters including central tendency (e.g. means) or other basic estimates (e.g. regression coefficient) AND variation (e.g. standard deviation) or associated estimates of uncertainty (e.g. confidence intervals)
☐	☒	For null hypothesis testing, the test statistic (e.g. *F*, *t*, *r*) with confidence intervals, effect sizes, degrees of freedom and *P* value noted *Give P values as exact values whenever suitable.*
☒	☐	For Bayesian analysis, information on the choice of priors and Markov chain Monte Carlo settings
☒	☐	For hierarchical and complex designs, identification of the appropriate level for tests and full reporting of outcomes
☒	☐	Estimates of effect sizes (e.g. Cohen's *d*, Pearson's *r*), indicating how they were calculated

Our web collection on statistics for biologists contains articles on many of the points above.

Software and code

Policy information about availability of computer code

Data collection	Confocal microscopy software: NIS-Elements AR version 5.21.02 Nano-indentation software: RiboScan version 10.0.0.21 SEM software: SmartSEM version 6.01 Rheology software: Rheology Advantage v5.8.2 Mechanical tests: Bluehill v.2
Data analysis	MS Excel 2019, Matlab 2018a, Origin Pro v8.5, R 3.6.0

For manuscripts utilizing custom algorithms or software that are central to the research but not yet described in published literature, software must be made available to editors and reviewers. We strongly encourage code deposition in a community repository (e.g. GitHub). See the Nature Research guidelines for submitting code & software for further information.

Data

Policy information about availability of data

All manuscripts must include a data availability statement. This statement should provide the following information, where applicable:

- Accession codes, unique identifiers, or web links for publicly available datasets
- A list of figures that have associated raw data
- A description of any restrictions on data availability

All relevant data are included in the paper and/or its Supplementary Information. All raw data are available from the authors on request.

Field-specific reporting

Please select the one below that is the best fit for your research. If you are not sure, read the appropriate sections before making your selection.

☒ Life sciences ☐ Behavioural & social sciences ☐ Ecological, evolutionary & environmental sciences

For a reference copy of the document with all sections, see nature.com/documents/nr-reporting-summary-flat.pdf

Life sciences study design

All studies must disclose on these points even when the disclosure is negative.

Sample size	Sample size was determined for each experiments as the minimum number of samples that guaranteed statistical significance of the measurements without making the study too complex to be handled
Data exclusions	We did not exclude data
Replication	We replicated the experiments and all the replicates provided data consistent with the one reported in the manuscript
Randomization	Samples allocation in experimental groups was randomized, i.e. seeds used for each coating treatment and control were randomly selected.
Blinding	As the results described are based on measurements of quantifiable parameters, blinding was not relevant for this study.

Reporting for specific materials, systems and methods

We require information from authors about some types of materials, experimental systems and methods used in many studies. Here, indicate whether each material, system or method listed is relevant to your study. If you are not sure if a list item applies to your research, read the appropriate section before selecting a response.

Materials & experimental systems

n/a	Involved in the study
☒	☐ Antibodies
☒	☐ Eukaryotic cell lines
☒	☐ Palaeontology and archaeology
☒	☐ Animals and other organisms
☒	☐ Human research participants
☒	☐ Clinical data
☒	☐ Dual use research of concern

Methods

n/a	Involved in the study
☒	☐ ChIP-seq
☒	☐ Flow cytometry
☒	☐ MRI-based neuroimaging